# Kittel Law in $BiFeO_3$ Ultrathin Films: A First-Principles-Based Study

S. Prosandeev,[1,*] S. Lisenkov,[2] and L. Bellaiche[1]

[1]*Physics Department, University of Arkansas, Fayetteville, Arkansas 72701, USA*
[2]*Department of Physics, University of South Florida, Tampa, Florida 33620, USA*

(Received 11 April 2010; published 28 September 2010)

A first-principles-based effective Hamiltonian is used to investigate the thickness dependency of the size of straight-walled domains in ultrathin films made of the multiferroic $BiFeO_3$ (BFO) material. It is found that the Kittel law is followed, as in ferroelectric or ferromagnetic films. However, an original real-space decomposition of the different energetic terms of this effective Hamiltonian allows the discovery that the microscopic origins of such a law in BFO films dramatically differ from those in ferroelectric or ferromagnetic films. In particular, interactions between tilting of oxygen octahedra around the domain walls and magnetoelectric couplings near the surface (and away from the domain walls) play an important role in the observance of the Kittel law in the studied BFO films.

DOI: 10.1103/PhysRevLett.105.147603 PACS numbers: 77.80.Dj, 75.85.+t, 77.55.Nv

Multiferroic thin films are attracting a lot of attention due to their promise in yielding original phenomena and applications, as a result of the coupling between electric and magnetic order parameters [1–3]. An important feature of such films is their domain structures and associated unusual characteristics [4–11]. For instance, Ref. [9] discovered that, surprisingly, domains in their grown $BiFeO_3$ (BFO) films do not follow the ''universal'' Kittel law (that states that the domain width is proportional to the square root of the sample's thickness [12,13]). This deviation from the Kittel law (KL) contrasts with the case of ferroelectric and ferromagnetic films [14], and was suggested to arise from the fact that the films of Ref. [9] have domains that are not straight but rather irregular in shape. However, it is presently unclear if KL can be obeyed even in BFO samples possessing straight-walled domains [10,11]. One reason for this paucity of knowledge is the small number of measured domain width-vs-thickness data and their large error bars [10,11]. Another reason is the likely strong effect of electrical boundary conditions on the measured domain period, as consistent with the observations that (i) for a given film's thickness, the domain period depends on the electrode on top of which the film is grown [11], and (ii) some BFO films increase, rather than decrease, their domain width when the film thickness decreases below a critical value [10,11]. Moreover, the microscopic interactions responsible for the observance or not of KL in multiferroic thin films are basically unknown.

The aims of this Letter are to use a first-principles-based technique, and to analyze its predictions via an original site-by-site energetic decomposition, to resolve the aforementioned issues in BFO. Our most important findings are (i) BFO thin films can indeed follow KL, and (ii) energetic terms responsible for KL in BFO films can dramatically differ from those leading to the observance of KL in ferroelectric and ferromagnetic films. In particular, we discovered that it is the competition between short-range interactions of tilting of oxygen octahedra at the domain walls vs the electric dipole-dipole interactions and magnetoelectric couplings at the surfaces (and away from the domain walls) that can give rise to KL in BFO films.

We use an effective Hamiltonian method to study (001) BFO films that are (i) experiencing an epitaxial strain of $-1.5\%$, (ii) under open-circuit electrical boundary conditions, and (iii) mimicked by supercells that are periodic along both $x$ and $y$ directions (chosen to be along the [100] and [010] directions) while finite along $z$ (that is parallel to [001]). Their total energy is

$$E_{\mathrm{tot}}(\{\mathbf{u}_i\},\{\eta\},\{\omega_i\},\{\mathbf{m}_i\}) = E_{\mathrm{FE\text{-}AFD}}(\{\mathbf{u}_i\},\{\eta\},\{\omega_i\}) + \sum_{i,j,\alpha,\gamma} Q_{ij,\alpha\gamma} m_{i,\alpha} m_{j,\gamma} + \sum_{i,j,\alpha,\gamma} D_{ij,\alpha\gamma} m_{i,\alpha} m_{j,\gamma} + \sum_{i,j,\alpha,\gamma,\nu,\delta} E_{ij,\alpha\gamma\nu\delta} m_{i,\alpha} m_{j,\gamma} u_{i,\nu} u_{i,\delta} + \sum_{i,j,\alpha,\gamma,\nu,\delta} F_{ij,\alpha\gamma\nu\delta} m_{i,\alpha} m_{j,\gamma} \omega_{i,\nu} \omega_{i,\delta} + \sum_{i,j,l,\alpha,\gamma} G_{ij,l,\alpha\gamma} \eta_l(i) m_{i,\alpha} m_{j,\gamma} + \sum_{i,l,\alpha,\gamma} B'_{l,\alpha\gamma} \eta_l(i) u_{i,\alpha} u_{i,\gamma} L^2 + \sum_{i,j} K_{ij} (\omega_{\mathbf{i}} - \omega_{\mathbf{j}}) \cdot (\mathbf{m}_{\mathbf{i}} \times \mathbf{m}_{\mathbf{j}}), \quad (1)$$

where $\alpha$, $\gamma$, $\nu$, and $\delta$ denote Cartesian components. The sums over $i$ run over all the Fe sites, while the sums over $j$ run over the first, second, and third nearest neighbors of the Fe site $i$—except for the second term where the sum over $j$ runs over all the Fe sites and the last term where the sum over $j$ only runs over the first nearest neighbors. $\mathbf{u}_i$ is the local soft-mode polar distortion in unit cell $i$. $\{\eta\}$ is the strain tensor [15], with $\eta_l(i)$ being its $l$th component (in Voigt notation) at the site $i$. $\omega_i$ characterizes the oxygen octahedron tilting—also termed the antiferrodistortive

 

(AFD) motions—in unit cell $i$. Its direction is the axis about which this octahedron tilts, while its magnitude provides the angle of such tilting. $\mathbf{m}_i$ is the magnetic dipole of cell $i$ and has a fixed magnitude of $4\mu_B$ [16]. $L^2$ is the magnitude square of the $G$-type antiferromagnetic vector.

$E_{\text{FE-AFD}}$ gathers the energetic terms associated with ferroelectricity (local self-energy, short-range and long-range interactions between electric dipoles), strain (elastic energy), and tiltings of oxygen octahedra (local self-energy and short-range interactions between AFD motions), and their mutual couplings. Its expression is the one provided in Ref. [17] except that the matrices describing the long-range electric dipolar interactions of bulks are replaced by those associated with two-dimensional systems under open-circuit (OC) electrical boundary conditions [18]. The second term of Eq. (1) represents the dipolar interactions between magnetic moments in films [18], while the third term characterizes the magnetic exchange interactions. The fourth, fifth, and sixth energies represent how local soft modes, AFD motions and strain, respectively, modify the exchange interactions [19]. The seventh and eight energetic terms were introduced [20] to reproduce the polarization's behavior of films under strain [21] and weak ferromagnetism observed in BFO films, respectively [22,23]. The parameters of Eq. (1) are extracted from first-principles calculations. Mechanical boundary conditions associated with the epitaxial growth on a (001) substrate are mimicked by freezing some components of the strain tensor [24,25]. The total energies of BFO films are used in Monte Carlo simulations, with up to $10^6$ sweeps. First-principles-based effective Hamiltonians successfully reproduced the structural ground state, magnetoelectric coefficients, and Néel and Curie temperatures of bulk BFO [19,20,26]. Moreover, effective Hamiltonians provided accurate size dependencies in ferroelectric films—including the observance of KL down to 3 unit cells [27–29].

In the present study, we consider specific 71° domains. Figures 1(a) and 1(b) display the local modes and the AFD-related vectors defined as $\mathbf{\Omega}_i = \boldsymbol{\omega}_i e^{-i\mathbf{k}\cdot\mathbf{r}_i}$, where $\mathbf{k} = \frac{\pi}{a} \times [111]$ (with $a$ being the pseudocubic lattice parameter) and $\mathbf{r_i}$ is the vector locating the center of cell $i$. (In the ground state of bulk BFO, the pattern exhibited by the $\mathbf{\Omega}_i$ vectors is homogeneous, reflecting the fact that the oxygen octahedra of any neighboring cell rotate in antiphase.) Such figures correspond to 10 K and a $\simeq 8$ nm-thick film. This 71° domain exhibits "up" and "down" nanostripes alternating along [100]. Inside the film [that is, away from the top and bottom four (001) $B$-layers], the up stripes possess $\mathbf{u}_i$ and $\mathbf{\Omega}_i$ vectors that are both mostly aligned along a $[uuv]$ direction, with $v > u$, while the down stripes are characterized by $\mathbf{u}_i$ and $\mathbf{\Omega}_i$ being both oriented along $[uu\text{-}v]$ [30] (the fact that the electric dipoles and AFD motions are along $\langle uuv \rangle$ directions arises from the compressive strain experienced by the film [21]). Figures 1(a) and 1(b) also reveal that, close to the surfaces, the electric dipoles and the AFD degrees of freedom form vortices,

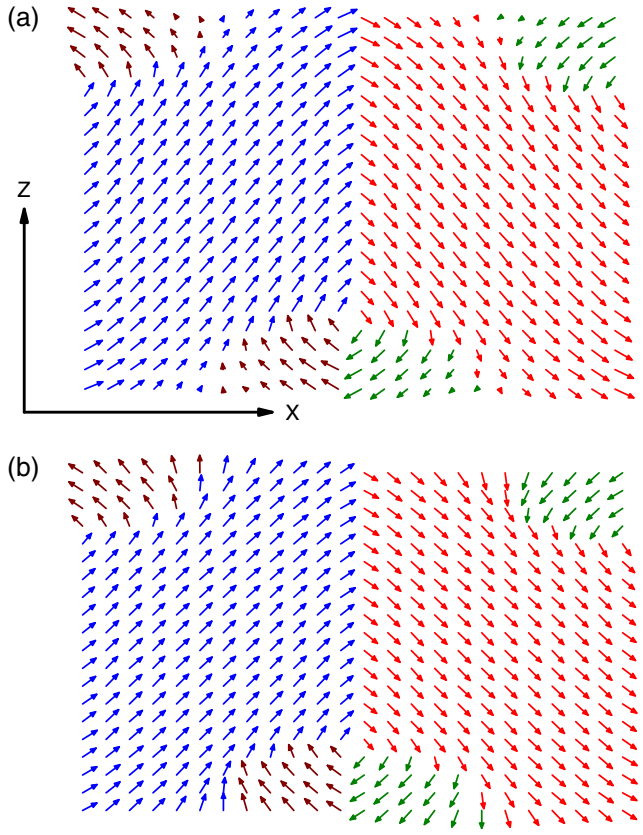


FIG. 1 (color online). 10 K pattern of the $\mathbf{u}_i$ local mode vectors [panel (a)] and $\mathbf{\Omega}_i$ AFD vectors [panel (b)] in a $(X, Z)$ plane for the equilibrium 71° domains of the 8 nm-thick film.

which is consistent with a recent experimental finding about toroidal patterns in BFO films [31]. Such formation leads to dipolar domain patterns possessing features of both Landau-Lifshitz [12] and Kittel [13] models in the sense that out-of-plane dipoles and flux-closure configurations both exist at the surfaces. We also found (not shown here) that, in addition to a homogeneous $G$-type antiferromagnetic vector, the BFO films adopt a weak ferromagnetic (FM) vector of the order of $0.03\mu_B$ inside each domain (this predicted magnitude is in excellent agreement with some measurements [23]). The direction of this FM vector varies between the up and down domains, as consistent with Ref. [4]. This change of direction arises from the facts that this FM vector desires to be perpendicular to the $\mathbf{\Omega}_i$'s and that $\mathbf{\Omega}_i$ rotates when going from the up to down domains.

Let us now investigate if KL is valid for these 71° domains. For that, we mimic different films by $N_x \times N_y \times h$ supercells, with $h$ (whose product by four provides the film thickness in angstroms) varying between 1 and 20. The in-plane supercell length along [010], $N_y$, is kept constant, while $N_x$ varies between 6 and 20 to find the equilibrium domain period for each thickness. Such an equilibrium period is denoted as $w_e$ in the following, and is the domain period yielding the lowest internal energy per 5-atom cell at low temperature [see Fig. 2(a)

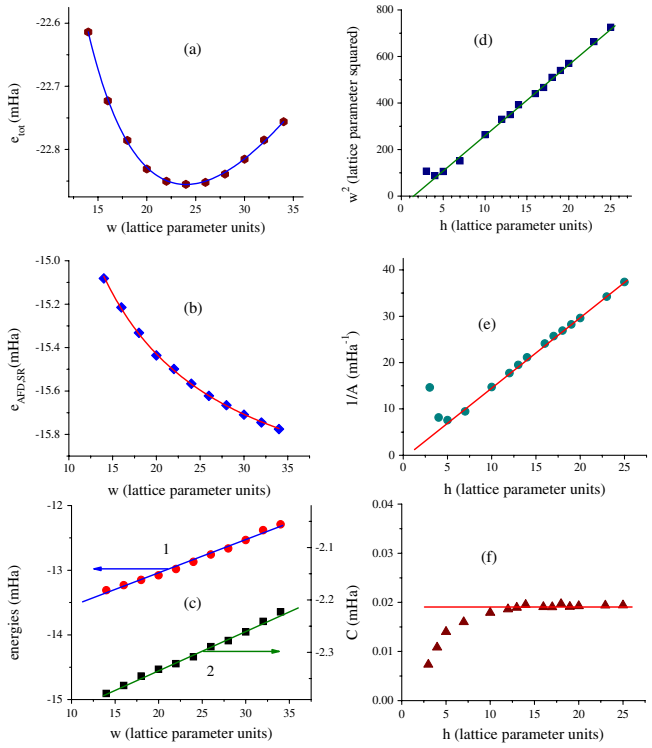


FIG. 2 (color online). Dependency of some energies [(a)–(c)] with domain period in 8 nm-thick films ($h = 20$), and thickness dependency of some features [(d)–(f)], at 10 K. The energy in (a) is the total internal energy per 5-atom cell provided by our simulations, with the solid line representing its fit by Eq. (2). The energy density shown in panel (b) is associated with the short-range interaction between AFD degrees of freedom. The two energy densities displayed in (c) correspond to the electric dipole-dipole interactions (curve 1) and the magnetoelectric interactions (curve 2). Panel (d) shows the square of the equilibrium domains period, while panels (e) and (f) display the $1/A$ and $C$ coefficients of Eq. (2), respectively.

for $h = 20$]. Figure 2(d) reveals that, for $h$ larger than 5, the square of $w_e$ is proportional to $h$. Our calculations thus confirms that KL can be obeyed in BFO films (above a critical thickness) if these latter exhibit stripe domains rather than fractal-like states [9,32]. Our predictions are also consistent with the (few and linear) $w_e^2$-versus-$h$ data of Ref. [11] for their 109° domains. Our predicted critical thickness below which KL breaks down corresponds to $h \sim 5$, and is thus of the same order as that of Pb(Zr, Ti)$O_3$ (PZT) and $PbTiO_3$ ferroelectric films (that is $h = 3$ [27–29]). The $w_e^2$-versus-$h$ curve of Fig. 2(d) has a slope around 31 (in units of the 5-atom-cell lattice parameter), to be compared with the value of 20 in PZT [27]. Furthermore, our studied domains were found to disappear for $h$ smaller than 3 (in favor, e.g., of a pure AFD state for $h = 1$), which is reminiscent of the vanishing of nanostripe domains in PZT and $BaTiO_3$ films for thickness below 12 Å [27].

The seminal papers of Landau-Lifshitz and Kittel [12,13] indicate that KL originates from the competition between an energy density that behaves as $1/w$ and another one that is proportional to $w$, where $w$ is the domains period. In other words, the total energy per 5-atom cell should be given by

$$e_{\text{tot}} = e_0 + Aw + \frac{C}{w}, \tag{2}$$

where $e_0$, $A$, and $C$ are all constant for a given film thickness. Interestingly, our computed total energy per 5-atom cell-vs-$w$ data can indeed be well fitted by Eq. (2) for any studied thickness—as revealed by Fig. 2(a) for the $h = 20$ film. Moreover, these fits for all the studied film thicknesses lead to the discovery that, for $h$ larger than 5, $1/A$ is linearly dependent on the film thickness [see Fig. 2(e)] while $C$ is merely independent of such thickness [see Fig. 2(f)]. In other words, $A = \frac{A_0}{h}$ and $C = C_0$ for thicknesses equal or larger than 20 Å, where $A_0$ and $C_0$ are constants and $h_0$ is of the order of 1.5 lattice constants. Minimizing the total energy density of Eq. (2) with respect to $w$, and inserting the aforementioned thickness dependence of $A$ and $C$ yield $w_e = \sqrt{C/A} = \sqrt{C_0(h - h_0)/A_0}$, that is, it provides KL. The computed ratio $C_0/A_0$ is around 31 lattice parameters, that is in excellent agreement with the slope of the linear function depicted in Fig. 2(d).

In the Landau-Lifshitz and Kittel's models, the energetic term that behaves as $1/w$ is the domain wall energy density, and involves the short-range dipolar interactions—because of the rotation of the dipole moments, when passing through the domain wall. On the other hand, the energy density that is proportional to $w$ is of a different nature in the two models: it is the anisotropy energy in the Landau-Lifshitz model (arising from the flux closure of dipoles at the surfaces) while it is the stray field (resulting from dipoles being out of plane at the surfaces) in the Kittel model. We numerically found that the main energetic term for which the energy density is inversely proportional to $w$ in our domains has nothing to do with short-range dipolar interactions. It is rather the short-range interactions between AFD motions (to be denoted by $e_{\text{AFD,SR}}$ for its energy density); see Fig. 2(b) for $h = 20$ [33]. We also determined that two specific energies have density that are linearly dependent on $w$. As shown in Fig. 2(c) for $h = 20$, they are the energy associated with electric dipole-dipole interactions and, to a smaller extent, the magnetoelectric interaction energy—that is the term involving the $E_{ij}$ coefficients in Eq. (1).

We also computed the site-by-site decomposition of these energies. Such decomposition is displayed in Figs. 3 for the equilibrium period of the $h = 20$ film. The energy corresponding to short-range interactions between AFD motions has a strong (costly) increase within the domain walls inside the whole film, revealing that the $1/w$ dependency of $e_{\text{AFD,SR}}$ microscopically originates from the domain walls (see Figs. 1 to identify regions associated with domain walls). On the other hand,

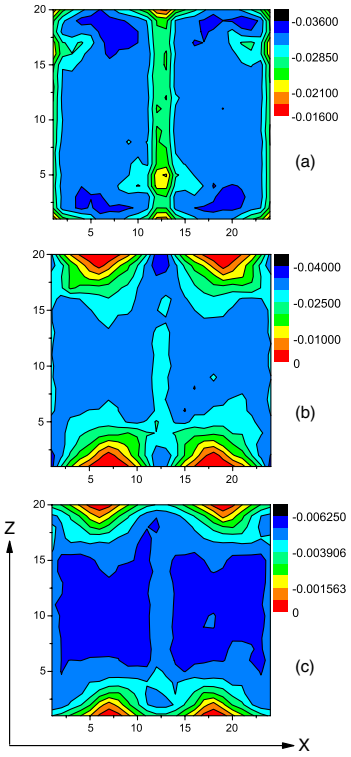


FIG. 3 (color online). 10 K site-by-site decomposition of the short-range interaction energy between AFD motions [panel (a)], electric dipole-dipole interactions [panel (b)] and magnetoelectric interaction energy [panel (c)] in the same $(X, Z)$ plane used for Fig. 1, for the equilibrium 71° domains of the 8 nm-thick film—as mimicked by a $24 \times 6 \times 20$ supercell.

the long-range interactions between electric dipoles are maximally costly away from the domain walls (i.e., within the up and down domains) at the surfaces. This finding is consistent with the stray fields of the Kittel model [13]. The energy representing the coupling between electric and magnetic dipoles is also maximally costly away from the domain walls, at the surface, because the local electric dipoles are the smallest in magnitude there [see Fig. 1(a)].

We hope that our study, revealing the validity of KL in BFO films and its unusual microscopic origins—as well as proposing a simple and efficient method, based on the site-by-site decomposition of the different energetics terms, to determine such origins and their real-space locations from atomistic simulations—will deepen the knowledge of the important fields of multiferroics and domains.

This work is supported by ONR Grants No. N00014-08-1-0915 and No. N00014-07-1-0825, DOE Grant No. DE-SC0002220, and NSF Grants No. DMR-0701558 and No. DMR-0080054. Computations were made possible thanks to the MRI NSF Grant No. 0722625 and to a Challenge grant from the U.S. DoD. S. L. acknowledges the support from the University of South Florida under Grant No. R074021. We thank H. Béa for useful discussions. S. P. appreciates Grants No. 08-02-92006NNSa and No. 09-02-92672INDa from RFBR.

*Also at Southern Federal University, 344090 Rostov on Don, Russia.

[1] M. Fiebig, J. Phys. D **38**, R123 (2005).
[2] D. I. Khomskii, J. Magn. Magn. Mater. **306**, 1 (2006).
[3] W. Eerenstein, N. D. Mathur, and J. F. Scott, Nature (London) **442**, 759 (2006).
[4] A. Lubk, S. Gemming, and N. A. Spaldin, Phys. Rev. B **80**, 104110 (2009).
[5] Y.-H. Chu *et al.*, Adv. Mater. **19**, 2662 (2007).
[6] Y.-H. Chu *et al.*, Nano Lett. **9**, 1726 (2009).
[7] L. W. Martin *et al.*, Nano Lett. **8**, 2050 (2008).
[8] F. Zavaliche *et al.*, Phase Transit. **79**, 991 (2006).
[9] G. Catalan *et al.*, Phys. Rev. Lett. **100**, 027602 (2008).
[10] Y. B. Chen *et al.*, Appl. Phys. Lett. **90**, 072907 (2007).
[11] C. W. Huang *et al.*, Phys. Rev. B **80**, 140101(R) (2009).
[12] L. Landau and E. Lifshitz, Phys. Z. Sowjetunion **8**, 153 (1935).
[13] C. Kittel, Phys. Rev. **70**, 965 (1946).
[14] G. Catalan, J. F. Scott, A. Schilling, and J. M. Gregg, J. Phys. Condens. Matter **19**, 022201 (2007).
[15] W. Zhong, D. Vanderbilt, and K. M. Rabe, Phys. Rev. Lett. **73**, 1861 (1994); Phys. Rev. B **52**, 6301 (1995).
[16] J. B. Neaton *et al.*, Phys. Rev. B **71**, 014113 (2005).
[17] I. Kornev *et al.*, Phys. Rev. Lett. **97**, 157601 (2006).
[18] I. Ponomareva *et al.*, Phys. Rev. B **72**, 140102(R) (2005); I. Naumov and H. Fu, arXiv:cond-mat/0505497.
[19] S. Lisenkov, I. A. Kornev, and L. Bellaiche, Phys. Rev. B **79**, 012101 (2009).
[20] D. Albrecht *et al.*, Phys. Rev. B **81**, 140401(R) (2010).
[21] A. J. Hatt, N. A. Spaldin, and C. Ederer, Phys. Rev. B **81**, 054109 (2010); B. Dupé *et al.*, Phys. Rev. B **81**, 144128 (2010).
[22] C. Ederer and N. A. Spaldin, Phys. Rev. B **71**, 060401(R) (2005).
[23] H. Béa *et al.*, Appl. Phys. Lett. **87**, 072508 (2005); H. Béa *et al.*, Philos. Mag. Lett. **87**, 165 (2007).
[24] I. Kornev, H. Fu, and L. Bellaiche, Phys. Rev. Lett. **93**, 196104 (2004).
[25] N. A. Pertsev, V. G. Kukhar, H. Kohlstedt, and R. Waser, Phys. Rev. B **67**, 054107 (2003).
[26] I. Kornev *et al.*, Phys. Rev. Lett. **99**, 227602 (2007).
[27] B. K. Lai *et al.*, Appl. Phys. Lett. **91**, 152909 (2007).
[28] S. K. Streiffer *et al.*, Phys. Rev. Lett. **89**, 067601 (2002).
[29] J. M. Gregg, Phys. Status Solidi A **206**, 577 (2009).
[30] The different directions of $\mathbf{u_i}$ and $\mathbf{\Omega}_i$ in the "up" and "down" domains lead to a finite polarization and a supercell average of the $\mathbf{\Omega}_i$ vectors that are both lying along an in-plane direction. On the other hand, the studied BFO ultrathin films do not possess any out-of-plane component of the polarization in order to vanish any depolarizing field. Our 71° domains thus differ from the 71° domains of Ref. [11] since these latter systems exhibit a nonzero polarization along the growth ($z$) direction.
[31] N. Balke *et al.*, Nature Nanotech. **4**, 868 (2009).
[32] The fractal states of Ref. [9] can transform into straight-walled domains [10,11] when growing the BFO films at a lower rate. H. Béa (private communication).
[33] In fact, the cost in energy associated with the short-range dipolar interactions is about twice as small as the cost in energy associated with short-range interactions between AFD motions. Moreover, the (positive) $1/w$ dependency of the short-range dipolar interactions is approximately fully compensated by the (negative) $1/w$ dependency of the local self-energy of the electric dipoles.